International Conference on Biomagnetism
2008, Sapporo, Japan, August 27, 2008

Adaptive Inverse Modeling: Current Status of Research and Future Directions

Kensuke Sekihara

Department of Systems Design & Engineering
Tokyo Metropolitan University

Outline of my talk

•Introduction of Adaptive Spatial-Filter Source Imaging

•Selected Topics on Adaptive Spatial Filters

(1) Imaging of induced activities

(2) Imaging of source coherence

•New Adaptive Algorithm beyond Adaptive Spatial Filters

Introduction to adaptive spatial-filter imaging

Spatial filter

Focused sensitivity

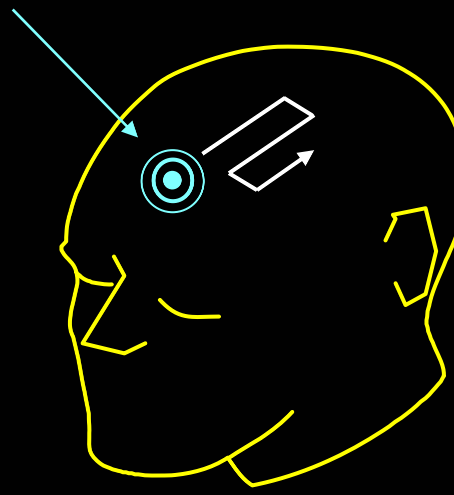

Spatial filter is a numerical technique that artificially focuses the sensitivity of the sensor array at a particular location.

Tomographic reconstruction

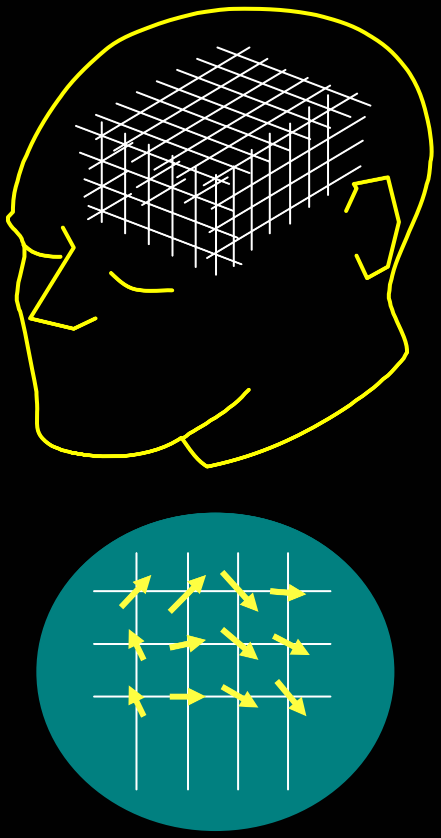

Definitions

data vector: $\boldsymbol{b}(t) = \begin{bmatrix} b_1(t) \\ b_2(t) \\ \vdots \\ b_M(t) \end{bmatrix}$

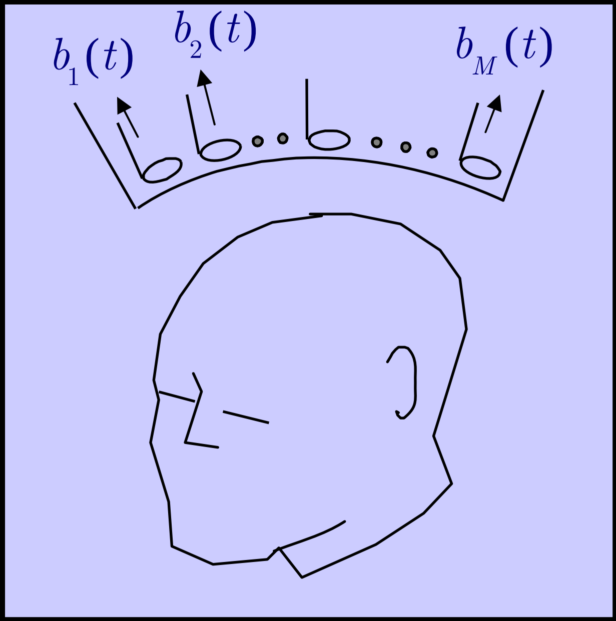

data covariance matrix: $\boldsymbol{R} = \left\langle \boldsymbol{b}(t)\boldsymbol{b}^T(t) \right\rangle$

source magnitude: $s(\boldsymbol{r},t)$

Sensor lead field

$$\boldsymbol{L}(\boldsymbol{r}) = \begin{bmatrix} l_1^x(\boldsymbol{r}) & l_1^y(\boldsymbol{r}) & l_1^z(\boldsymbol{r}) \\ l_2^x(\boldsymbol{r}) & l_2^y(\boldsymbol{r}) & l_2^z(\boldsymbol{r}) \\ \vdots & \vdots & \vdots \\ l_M^x(\boldsymbol{r}) & l_M^y(\boldsymbol{r}) & l_M^z(\boldsymbol{r}) \end{bmatrix}$$

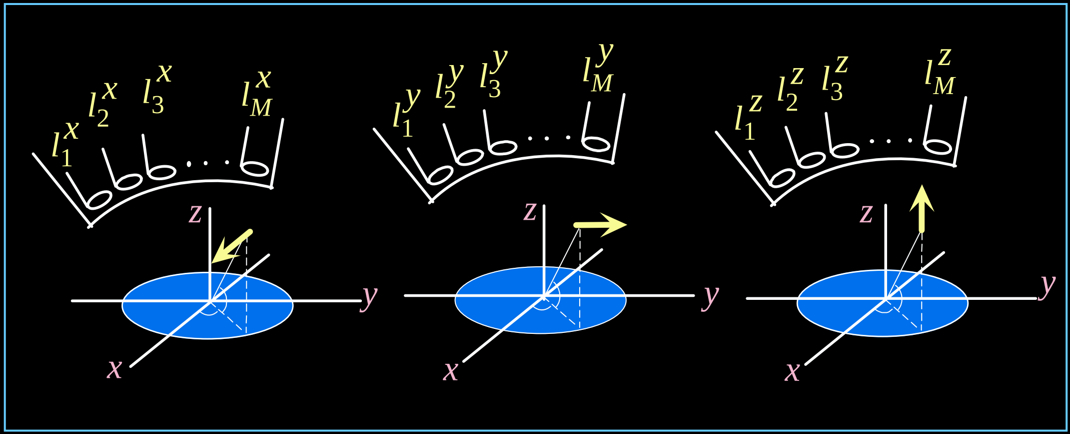

$$\boldsymbol{l}(\boldsymbol{r}) = \boldsymbol{L}(\boldsymbol{r})\boldsymbol{\eta}(\boldsymbol{r})$$

Spatial filter-basic formulation

weight vector

↓

$$\hat{s}(\boldsymbol{r},t) = \boldsymbol{w}^T(\boldsymbol{r})\boldsymbol{b}(t) = [w_1(\boldsymbol{r}),\ldots,w_M(\boldsymbol{r})]\begin{bmatrix} b_1(t) \\ \vdots \\ b_M(t) \end{bmatrix} = \sum_{m=1}^{M} w_m(r) b_m(t)$$

↑

Estimate of source activity

Non-adaptive spatial filter:

$\boldsymbol{w}(\boldsymbol{r})$ is data independent

Adaptive spatial filter:

$\boldsymbol{w}(\boldsymbol{r})$ is data dependent

Minimum-variance filter

Weight derivation

$$\boldsymbol{w} = \arg\min_{\boldsymbol{w}} \boldsymbol{w}^T \boldsymbol{R} \boldsymbol{w} \text{ subject to } \boldsymbol{w}^T \boldsymbol{l}(\boldsymbol{r}) = 1$$

$$\Downarrow$$

$$\boldsymbol{w}(\boldsymbol{r}) = \boldsymbol{R}^{-1}\ \boldsymbol{l}(\boldsymbol{r}) / [\boldsymbol{l}^T(\boldsymbol{r})\boldsymbol{R}^{-1}\boldsymbol{l}(\boldsymbol{r})]$$

Robinson and Rose, Biomagnetism: Clinical Aspects, Elsevier Science Publishers, 1992

Minimum-variance filter for unknown source orientation

$$\boldsymbol{\eta}_{opt} = \arg\min_{\boldsymbol{\eta}} \left(\boldsymbol{\eta}^T [\boldsymbol{L}^T(\boldsymbol{r})\boldsymbol{R}^{-1}\boldsymbol{L}(\boldsymbol{r})]\boldsymbol{\eta} \right) = \boldsymbol{u}_{min}$$

$\uparrow$

Eigenvector corresponding to the minimum eigenvalue of $[\boldsymbol{L}^T(\boldsymbol{r})\boldsymbol{R}^{-1}\boldsymbol{L}(\boldsymbol{r})]$

$$\boldsymbol{w}(\boldsymbol{r}) = \frac{\boldsymbol{R}^{-1}\ \boldsymbol{l}(\boldsymbol{r})}{[\boldsymbol{l}^T(\boldsymbol{r})\boldsymbol{R}^{-1}\boldsymbol{l}(\boldsymbol{r})]}, \text{ where } \boldsymbol{l}(\boldsymbol{r}) = \boldsymbol{L}(\boldsymbol{r})\boldsymbol{u}_{min}$$

Orientation estimation: Sekihara et al., Biomag 96:Proceedings of the Tenth International Conference on Biomagnetism, Santa Fe, Feb. 1996

High spatial resolution of adaptive spatial filter

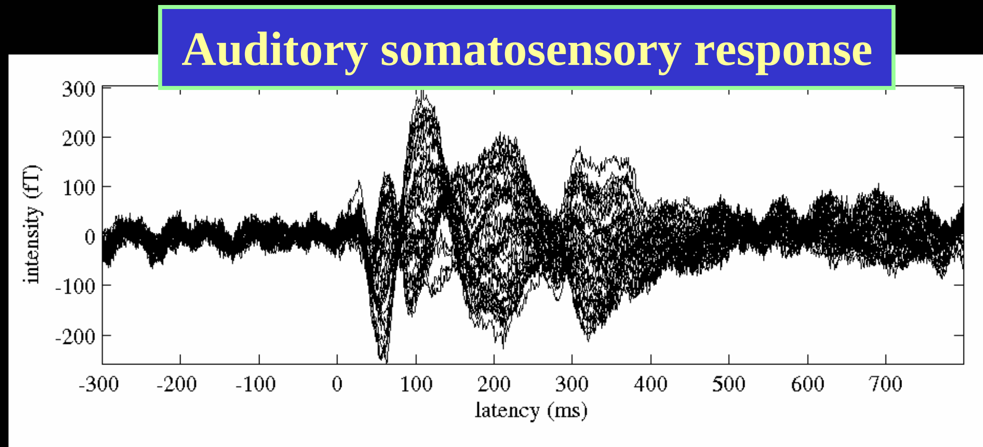

Minimum-variance filter

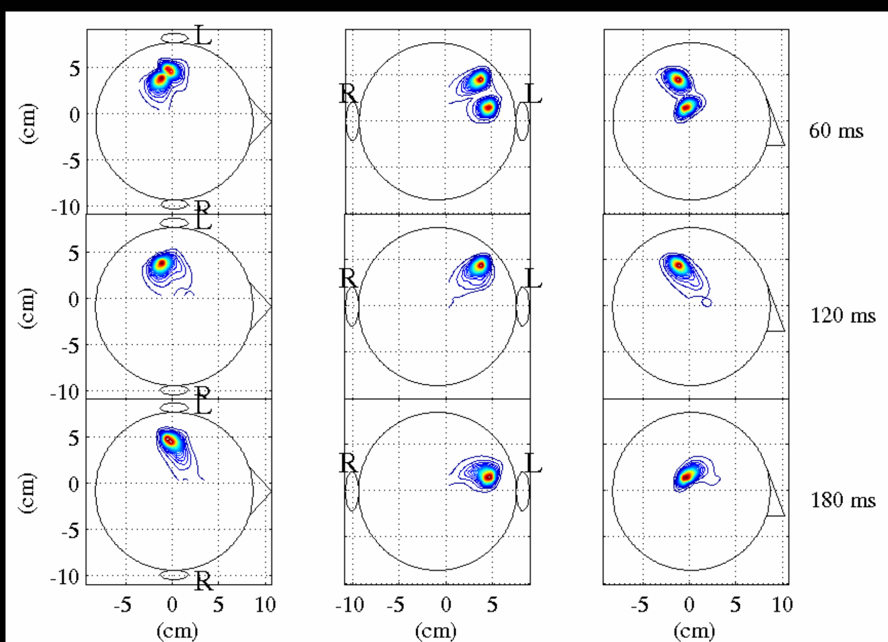

sLORETA

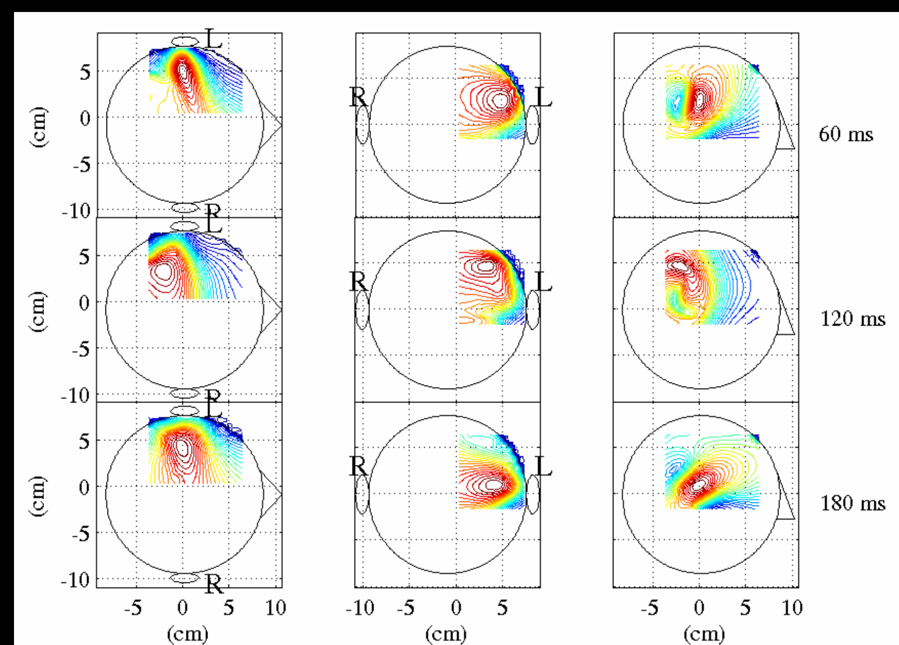

Summary of our work on adaptive spatial filters

- Source orientation estimation by minimum-variance spatial filter

  K. Sekihara, B Scholz, Proceedings of Biomag 96, Springer Verlag, 1996.

- Array mismatch problem and eigenspace projection

  K. Sekihara, S. S. Nagarajan, D. Poeppel, A. Marantz, Y. Miyashita, Human Brain Mapping, Vol. 15, 2002
  Sekihara, K. Nagarajan, S.S. Poeppel, D. Marantz, A. Miyashita, Y., IEEE Trans Biomed Eng., Vol.48, 2001

- Correlated source influence and region suppression beamformer

  Sekihara K., Nagarajan S.S., Poeppel D., Marantz A., IEEE Trans Biomed Eng. Vol.49,2002.
  Dalal SS, Sekihara K, Nagarajan SS, IEEE Trans Biomed Eng. Vol.53, 2006.

- Asymtotic SNR and equivalence of vector vs scalar spatial filters

  Sekihara K., Nagarajan S.S., Poeppel D., Marantz A., IEEE Trans Biomed Eng. Vol.51, 2004.

- Effects of low and high rank interferences

  Sekihara K., Nagarajan S.S., Poeppel D., Marantz A., IEEE Trans Biomed Eng. Vol.51(1), 2004.
  Sekihara K, Hild KE, Nagarajan SS. , IEEE Trans Biomed Eng. Vol.53(9), 2006.
  Sekihara K, Hild KE, Salal, SS, Nagarajan SS. , IEEE Trans Biomed Eng. Vol.55(3), 2008.

- Bias and spatial Resolution: comparison to non-adaptive spatial filters

  K. Sekihara, M. Sahani, S.S. Nagarajan, NeuroImage, Vol.25, 2005.

- Statistical thresholding of spatial-filter images

  K. Sekihara, M. Sahani, S.S. Nagarajan, NeuroImage, Vol.27, 2005.

- NUTMEG toolbox

  S. S. Dalal, J. M. Zumer, V. Agrawal, K. E. Hild, K. Sekihara, S. S. Nagarajan, Neurology and Clinical neurophysiology, Vol.52, 2004.

- Time-frequency source imaging

  Dalal S.S., Guggisberg A.G., Edwards E., Sekihara K., et al., Neuroimage. 2008 May 1;40(4):1686-700.

- Introduction of Adaptive Spatial-Filter Source Imaging

- Selected Topics on Adaptive Spatial Filters

    (1) Imaging of induced activities

    (2) Imaging of source coherence

- New Adaptive Algorithm beyond Adaptive Spatial Filters

Induced activity

Task-related modulation of oscillatory brain activity

Induced activity:

- Stimulus-evoked but not phase-locked to the stimulus
- frequency specific

↓

Event-related power change

Power decrease → Event-related desynchronization (ERD)

Power increase → Event-related synchronization (ERS)

G. Pfurtscheller and F. H. Lopes da Silva: "Event-related EEG/MEG synchronization and desynchronization: basic principles," Clin. Neurophysiol., 1997

Induced activity may not be detected in averaged results

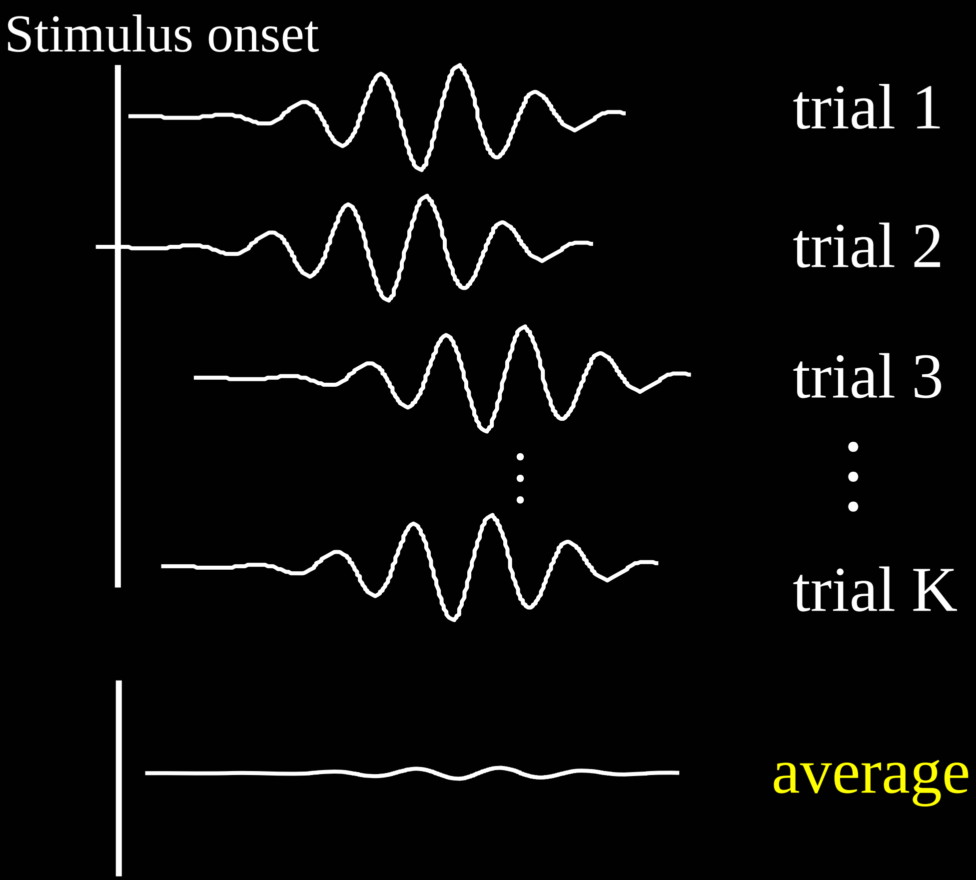

Induced activity has time jitter

Motor-evoked MEG
100-trial-averaged results

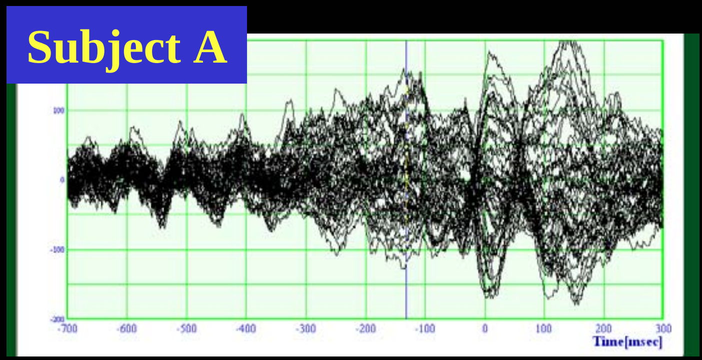

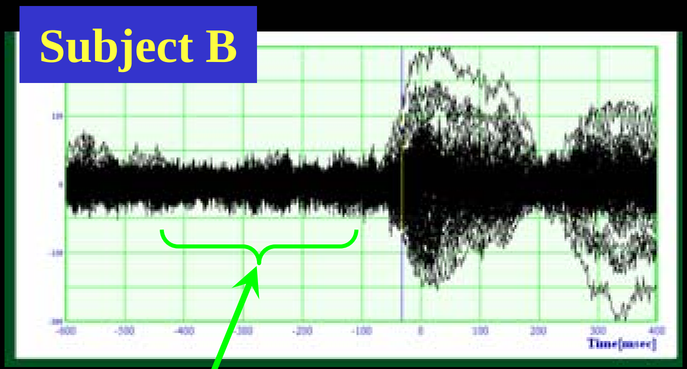

No clear premotor response exists in average waveform

Covariance matrix must be computed from non-averaged trials

Stimulus onset

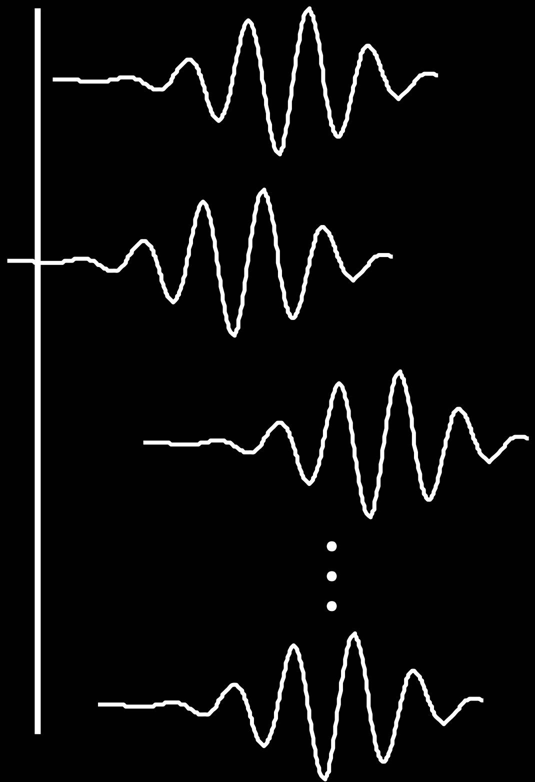

trial 1 $\Rightarrow \boldsymbol{R}_1$

trial 2 $\Rightarrow \boldsymbol{R}_2$

trial 3 $\Rightarrow \boldsymbol{R}_3$

⋮

trial K $\Rightarrow \boldsymbol{R}_K$

$$\boldsymbol{R} = \sum_{j=1}^{K} \boldsymbol{R}_j$$

This R contains unwanted background interference

Influence of background source activity
(Influence of brain noise)

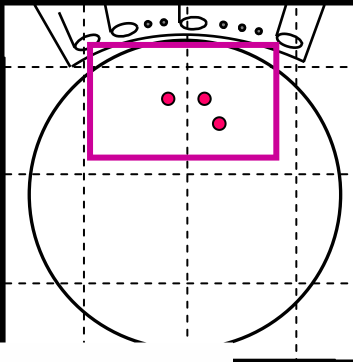

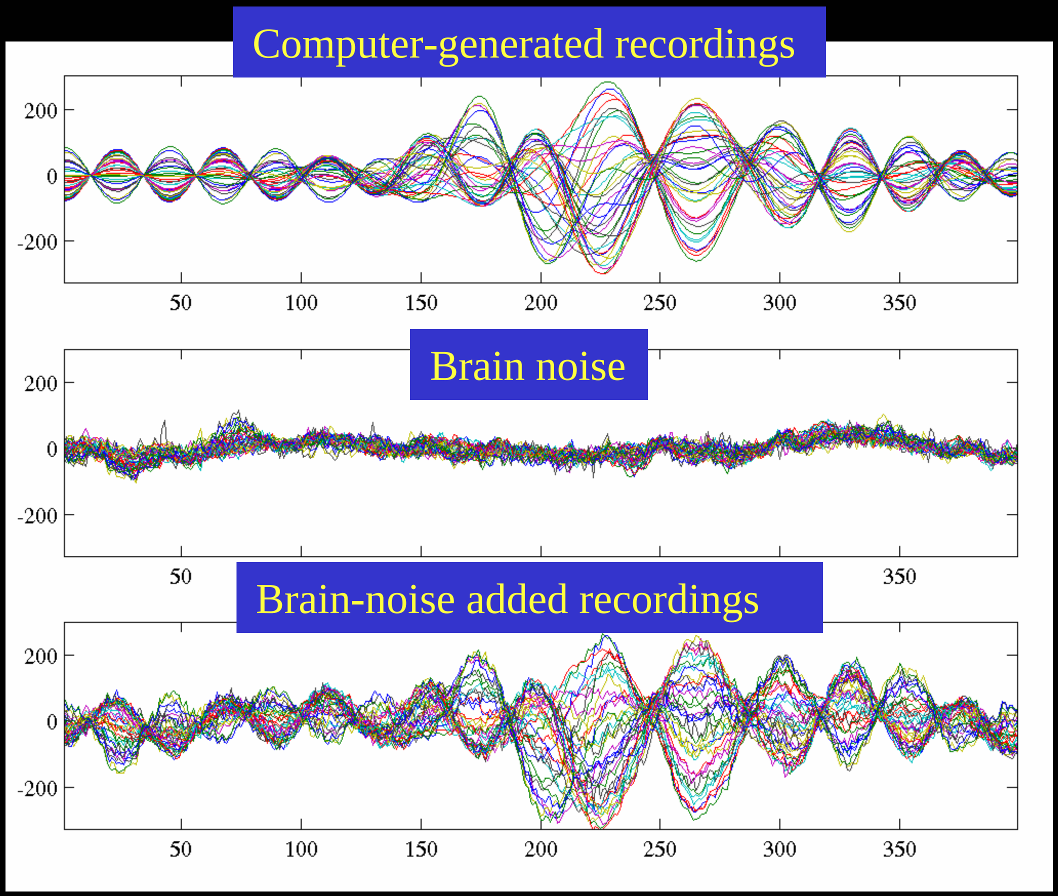

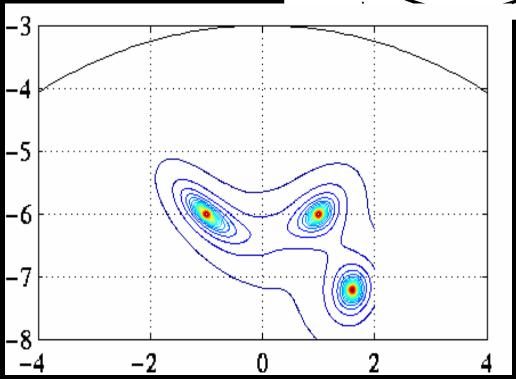

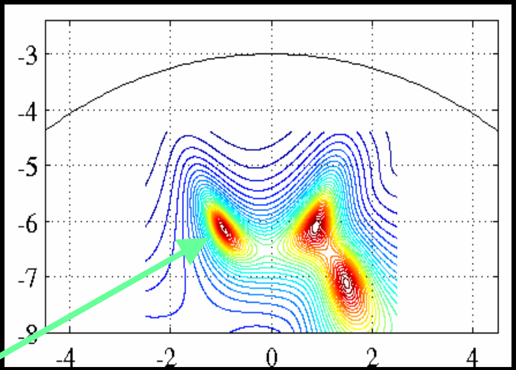

Background activity causes a severe blur.

Dual-condition experiments

Task: $\boldsymbol{b}(t) = \boldsymbol{b}_S(t) + \boldsymbol{b}_I(t) + \boldsymbol{n}(t)$

Control: $\boldsymbol{b}_C(t) = \boldsymbol{b}_I(t) + \boldsymbol{n}(t)$

↓

Covariance matrix relations

Task: $\boldsymbol{R} = \boldsymbol{R}_S + \boldsymbol{R}_{i+n}$

Control: $\boldsymbol{R}_C = \boldsymbol{R}_{i+n}$

Problem:

How to obtain interference-free source reconstruction by using the task data $\boldsymbol{b}(t)$ and the control data $\boldsymbol{b}_c(t)$

Existing approach: image-based subtraction

Define $s(\boldsymbol{r})$: source image from $\boldsymbol{b}(t)$

$s_c(\boldsymbol{r})$: source image from $\boldsymbol{b}_c(t)$

Calculate $\Delta s(\boldsymbol{r}) = s(\boldsymbol{r}) - s_c(\boldsymbol{r})$

Robinson's *F* ratio method

$$F(\boldsymbol{r}) = \frac{\left\langle s(\boldsymbol{r})^2 \right\rangle - \left\langle s_C(\boldsymbol{r})^2 \right\rangle}{\left\langle s_C(\boldsymbol{r})^2 \right\rangle}$$

This approach works when SIR is high, but becomes less effective when large brain noise exists, because the influence of brain noise is not simply additive.

S. E. Robinson and J. Vrba, Recent Advances in Biomagnetism, pp. 302-305, 1999

Prewhitening estimation of signal covariance R_S

Task:	$\boldsymbol{R} = \boldsymbol{R}_S + \boldsymbol{R}_{i+n}$
Control:	$\boldsymbol{R}_C = \boldsymbol{R}_{i+n}$

$\Rightarrow$ Calculate $\tilde{\boldsymbol{R}} = \boldsymbol{R}_C^{-1/2}\boldsymbol{R}\boldsymbol{R}_C^{-1/2}$

Signal covariance estimation

$$\hat{\boldsymbol{R}}_S = \boldsymbol{R}_C^{1/2}\left[\boldsymbol{U}_S\boldsymbol{U}_S^T(\tilde{\boldsymbol{R}} - \boldsymbol{I})\right]\boldsymbol{R}_C^{1/2} = \boldsymbol{R}_C^{1/2}\left[\sum_{j=1}^{Q}(\gamma_j - 1)\boldsymbol{u}_j\right]\boldsymbol{R}_C^{1/2}$$

$\uparrow$

$\boldsymbol{U}_S = [\boldsymbol{u}_1, \ldots, \boldsymbol{u}_Q]$: signal-level eigenvectors of $\tilde{\boldsymbol{R}}_S$

Prewhitening spatial filter

use $\hat{\boldsymbol{R}}_S$ for computing the filter weight

$$\boldsymbol{w}(\boldsymbol{r}) = \hat{\boldsymbol{R}}_S^{-1}\,\boldsymbol{l}(\boldsymbol{r}) / [\boldsymbol{l}^T(\boldsymbol{r})\hat{\boldsymbol{R}}_S^{-1}\boldsymbol{l}(\boldsymbol{r})]$$

Sekihara K, et al. IEEE Trans Biomed Eng. 2006 Mar;53(9).

Sekihara K, et al. IEEE Trans Biomed Eng. 2008 Mar;55(3).

Frequency-domain adaptive spatial filter

Because the induced signal is frequency specific, another strategy that further reduces the brain-noise-influence is to use the weight tuned to the frequency of the induced signal.

Frequency-specific weight

$\boldsymbol{R}(f)$: Covariance matrix calculated from the frequency band of the induced signal.

$$\boldsymbol{w}(f) = \boldsymbol{R}(f)\,\boldsymbol{l}(\boldsymbol{r})\,/\,[\boldsymbol{l}^T(\boldsymbol{r})\boldsymbol{R}(f)\,\boldsymbol{l}(\boldsymbol{r})],$$

This frequency-specific weight is used together with the prewhitening method in the following experiments.

Results of frequency-specific-prewhitening filter for hand-motor measurement

Voluntary right-finger movement (every 10 sec)

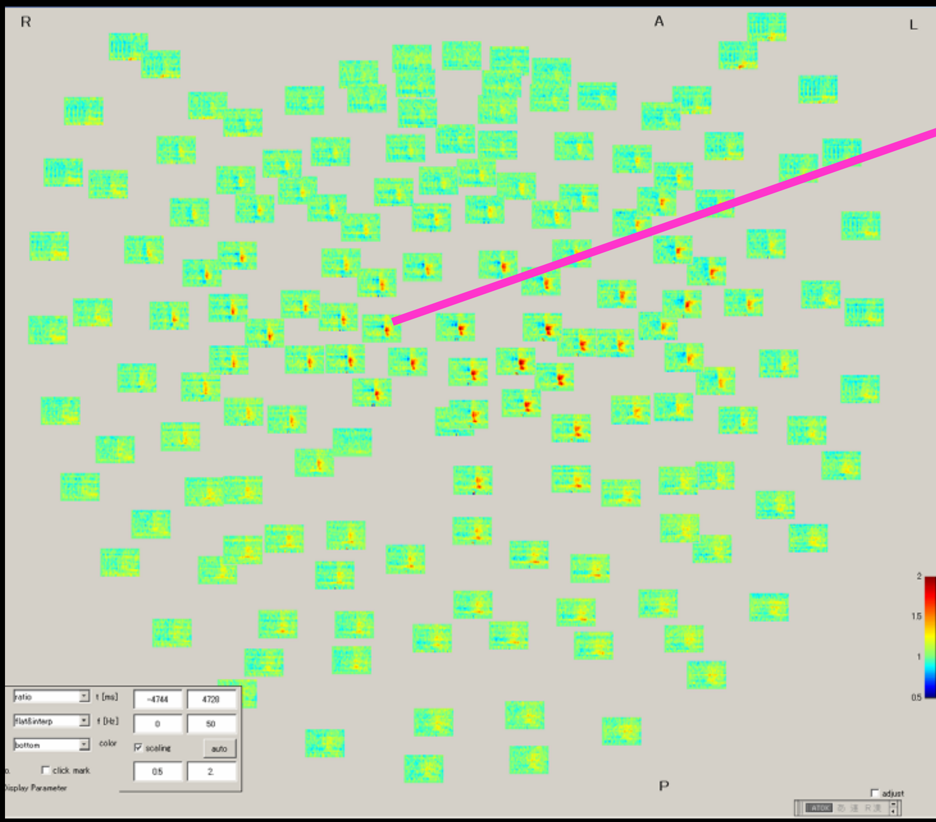

TF maps of data from all sensors

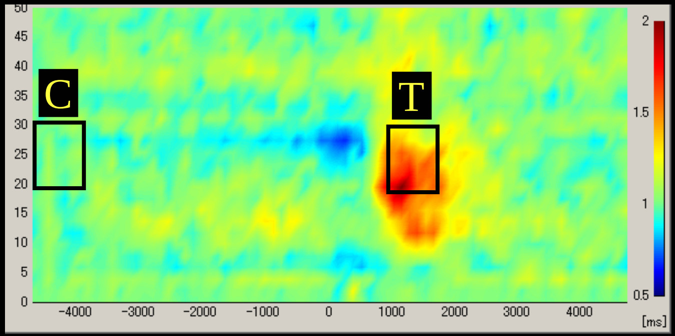

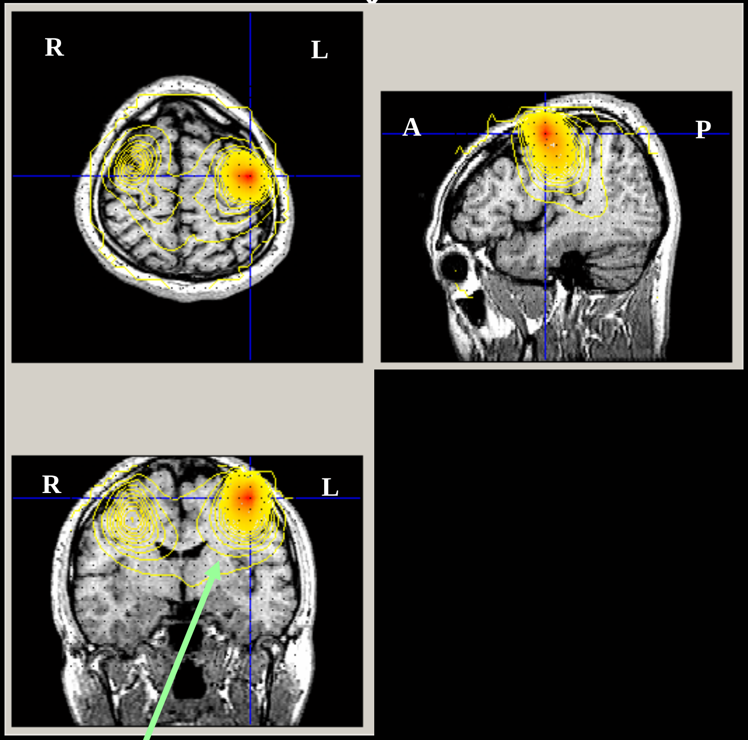

A localized source is found near contra-lateral M1 area

Comparison between prewhitening and F-image methods

MRI overlay

Prewhitening results

F image results

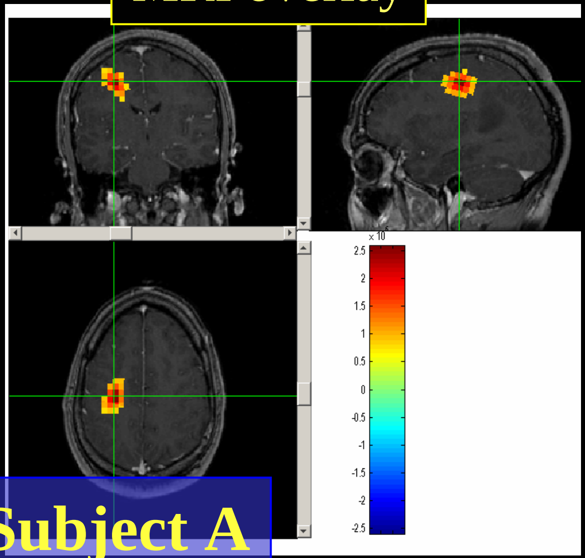

Subject A

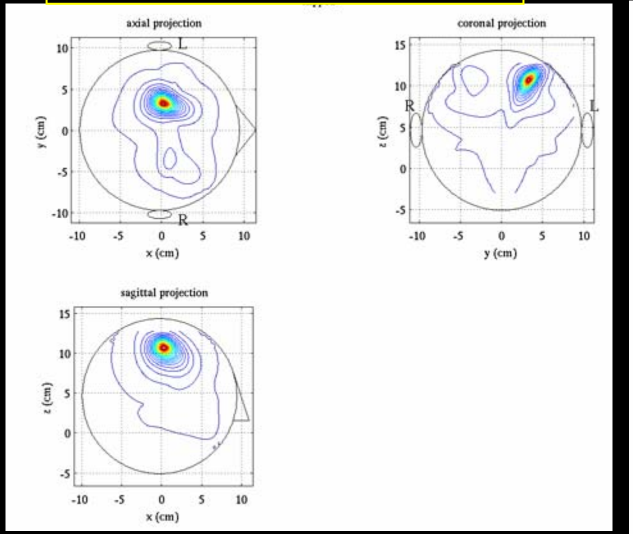

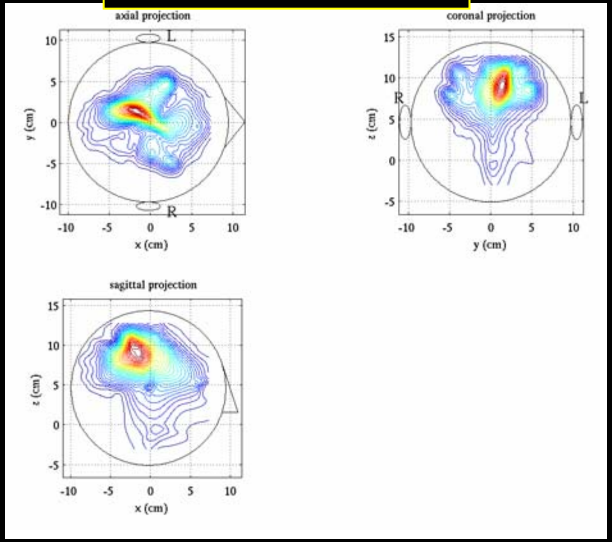

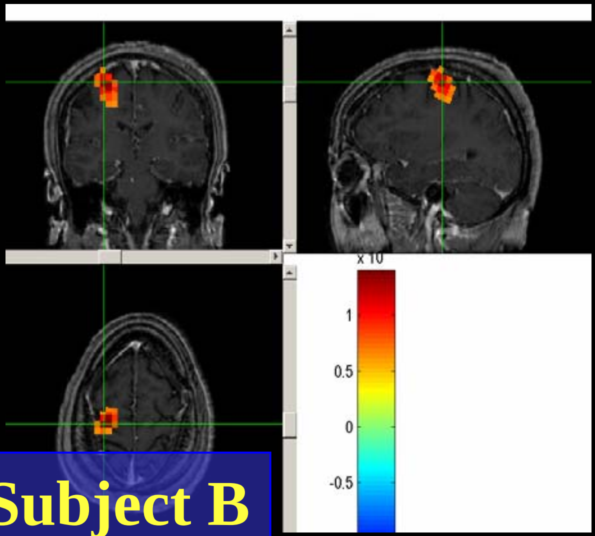

Subject B

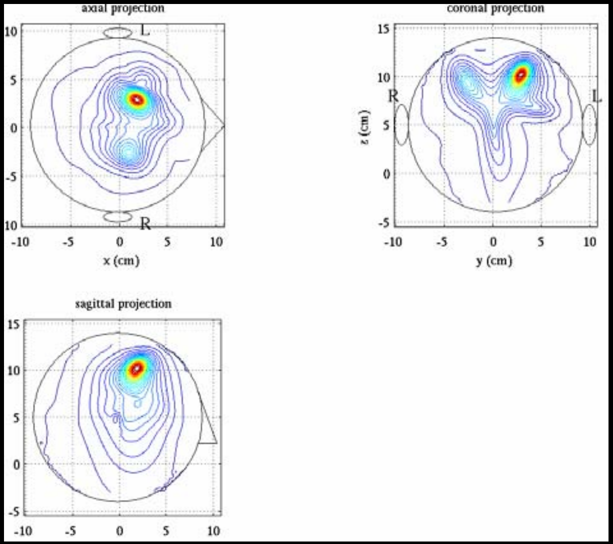

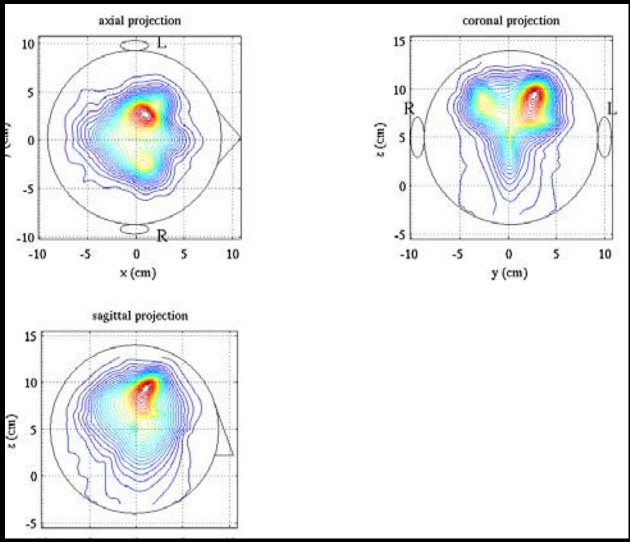

Sekihara K, et al. IEEE Trans Biomed Eng. 2006 Mar;53(9).

Spike-locked dual-state adaptive spatial filter

Spike sources are localized using the beta- and gamma-band power change accompanying interictal epilectic spikes

Multiple data portions each containing a spike are collected from total 60-minites continuous, interictal, resting state MEG recordings.

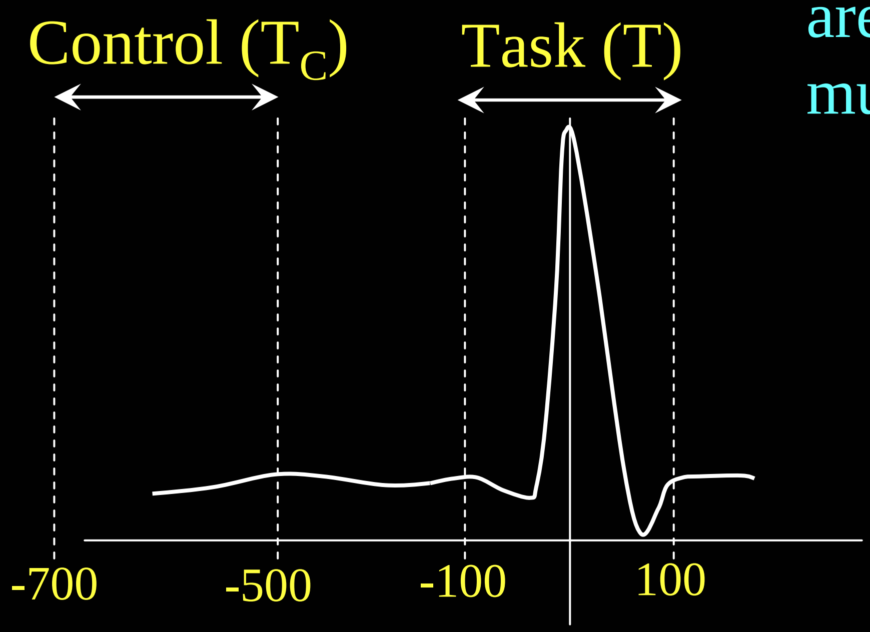

Control and task covariance matrices are calculated by averaging across multiple spike data sets:

$$\boldsymbol{R}_C = \sum_{\text{spikes}} \sum_{f \in F_W} \boldsymbol{R}(f, T_C)$$

$$\boldsymbol{R} = \sum_{\text{spikes}} \sum_{f \in F_W} \boldsymbol{R}(f, T)$$

F_W :12-55Hz

A. G. Guggisberg *et al*., NeuroImage Vol.39, 2008

Results

Time-frequency maps

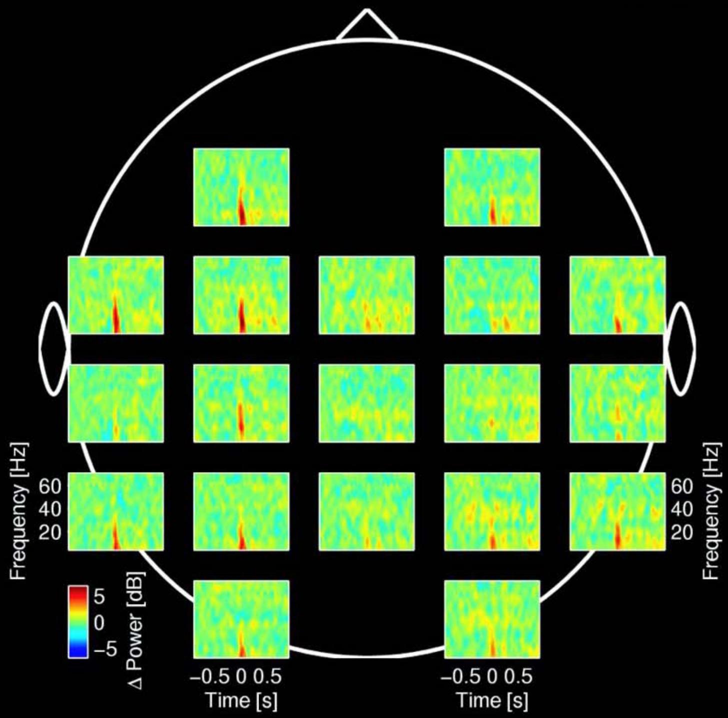

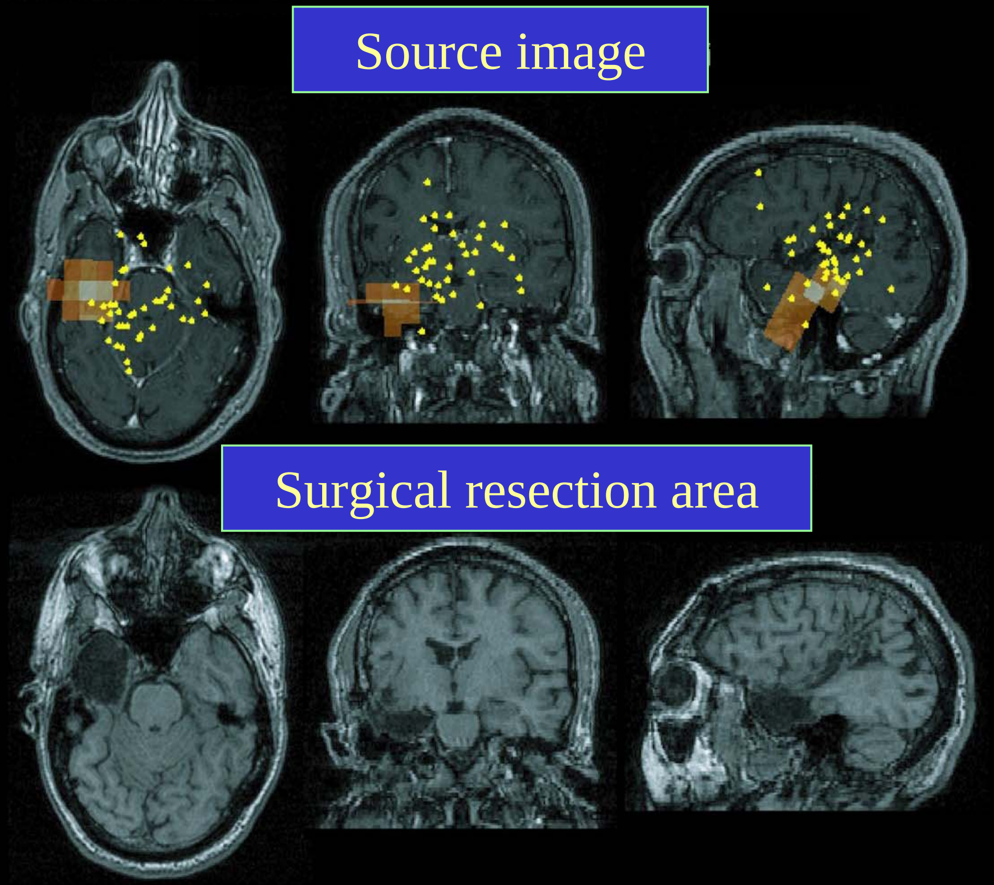

The surgical resection area was determined by interoperative ECoG recordings and extraoperative subdural ictal ECoG recordings when needed. **Thus, the resection area accurately shows the epileptogenic zone and can work as a gold standard for assessing the imaging results.**

A. G. Guggisberg *et al*., NeuroImage Vol.39, 2008

Dual-state spatial filter can be extended to time-frequency reconstruction of source activity

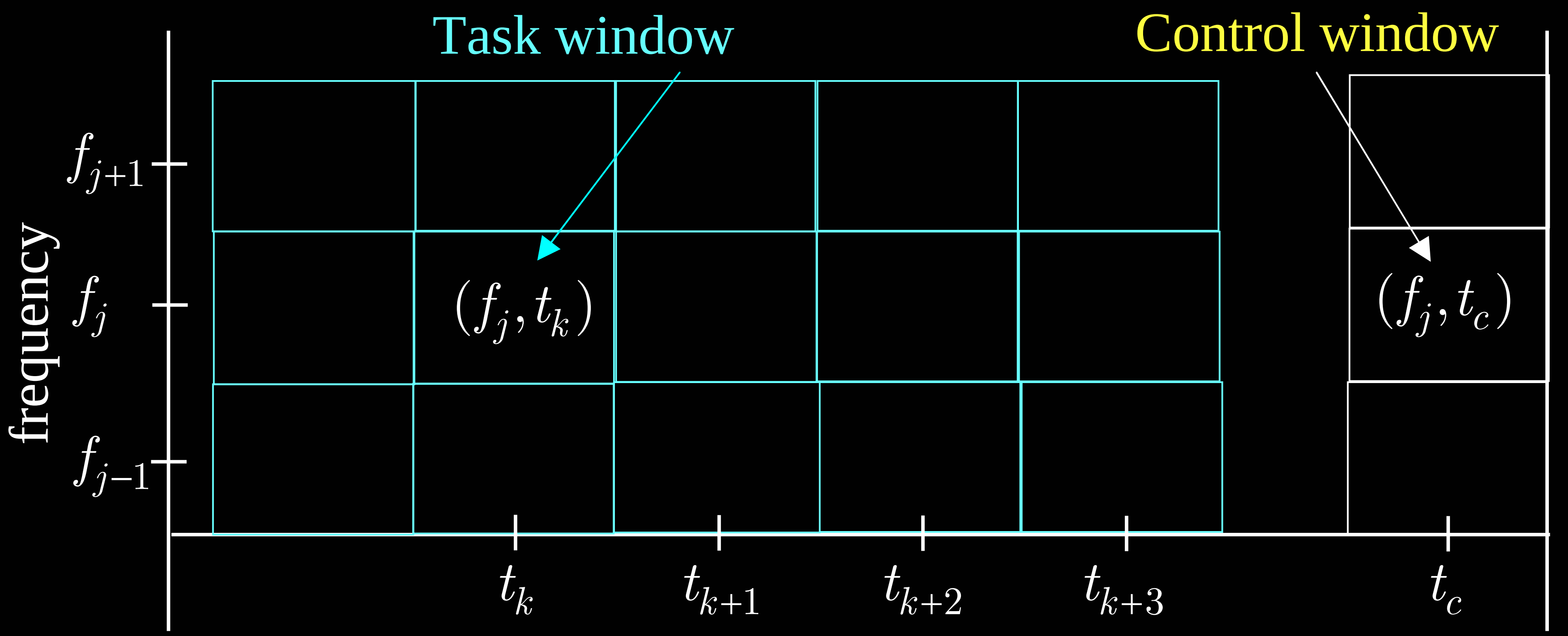

$s(\boldsymbol{r}, f_j, t_k)$: source reconstruction by setting the task window at (f_j, t_k) and control window at (f_j, t_c).

A set of $s(\boldsymbol{r}, f_j, t_k)$: $j = 1, 2, \ldots$: $k = 1, 2, \ldots$ represents time-frequency reconstruction of source activity.

Five dimensional imaging from hand-motor data

Beta-band activity

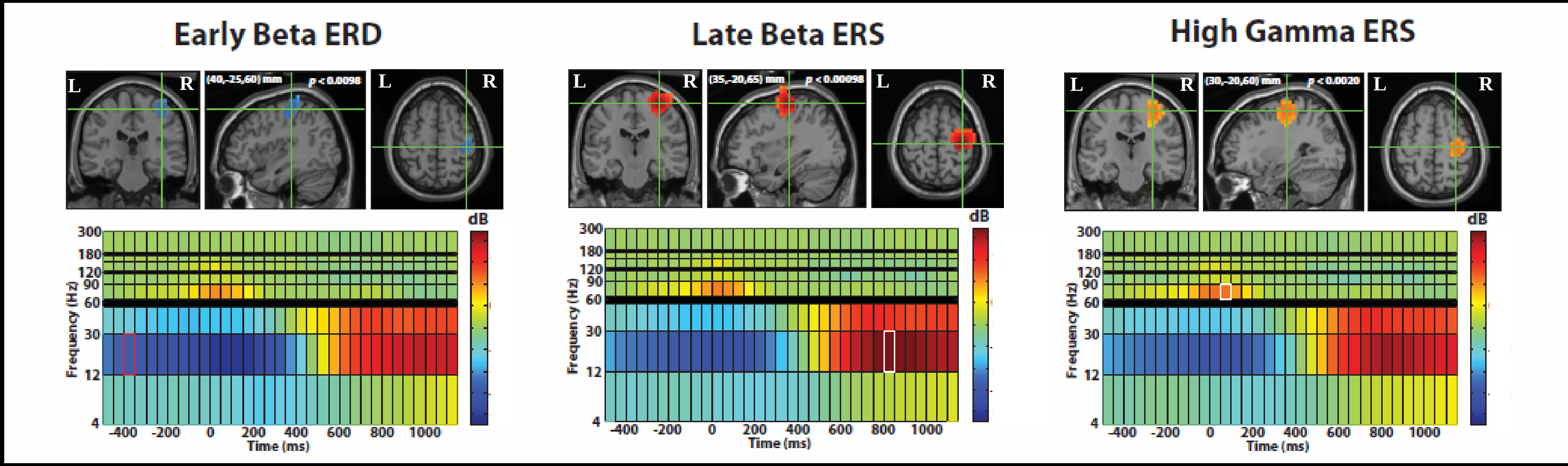

High-gamma-band activity

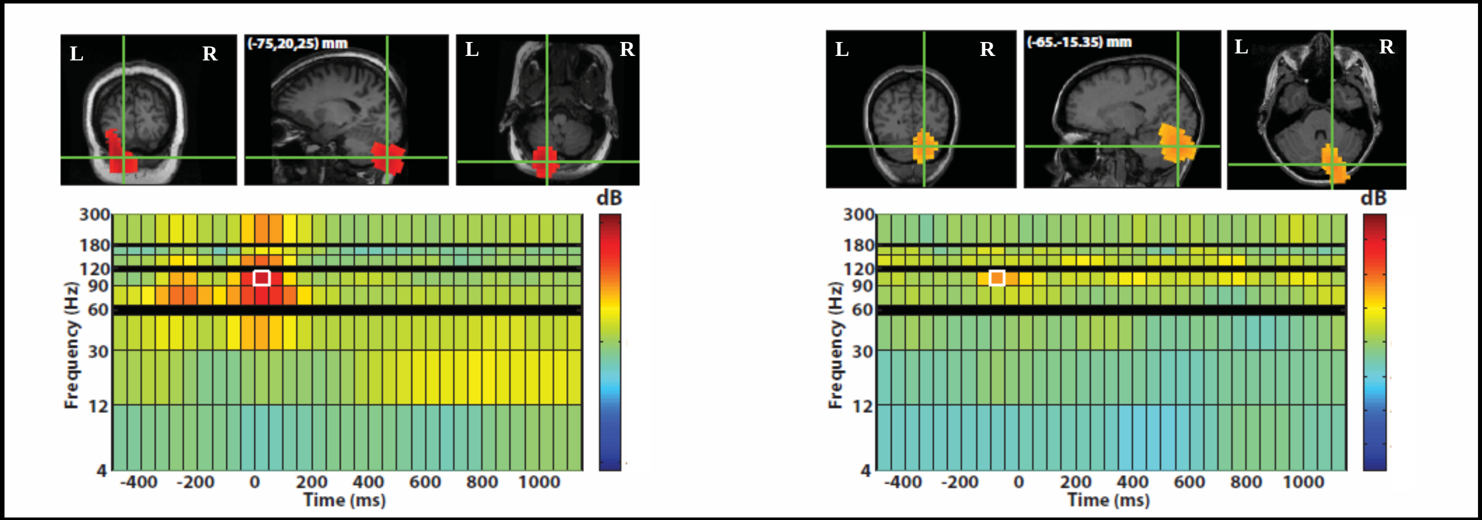

Dalal S.S., Guggisberg A.G., Edwards E., Sekihara K., et al., Neuroimage. 2008 May 1;40(4):1686-700.

Comparison with ECoG results

Right finger (RD2) movement

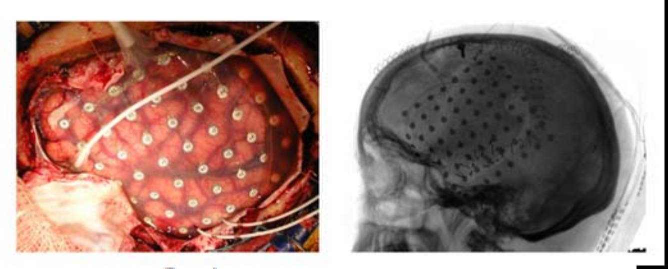

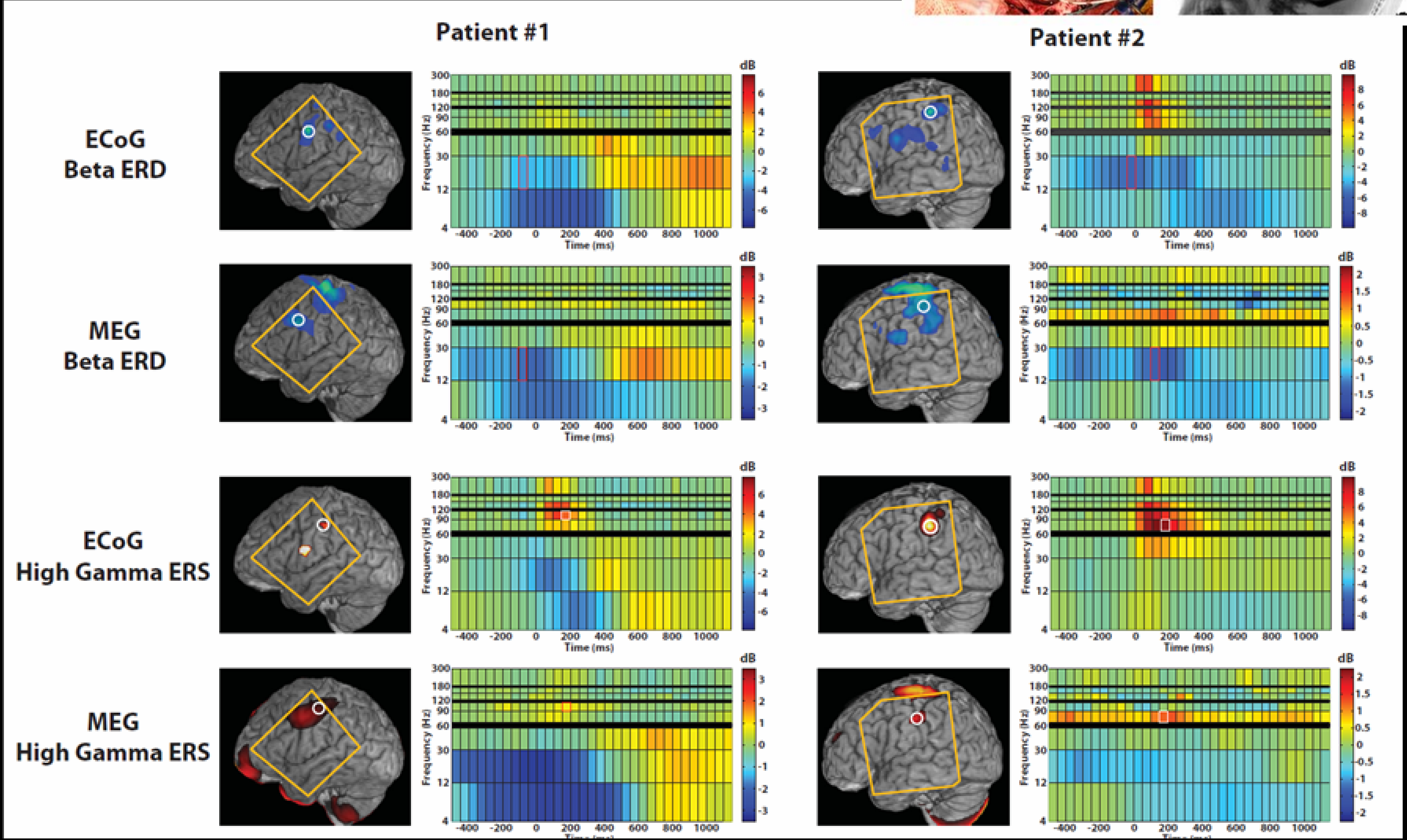

Dalal S.S., Guggisberg A.G., Edwards E., Sekihara K., et al., Neuroimage. 2008 May 1;40(4):1686-700.

- Introduction of Adaptive Spatial-Filter Source Imaging

- Selected Topics on Adaptive Spatial Filters

  (1) Imaging of induced activities

  (2) Imaging of source coherence

- New Adaptive Algorithm beyond Adaptive Spatial Filters

Imaging of cortical source coherence/brain interaction

DICS algorithm

Coherence between $\boldsymbol{r}_i$ and $\boldsymbol{r}_j$:

$$\eta(f, \boldsymbol{r}_i, \boldsymbol{r}_j) = \frac{\boldsymbol{w}(\boldsymbol{r}_i, f)\boldsymbol{R}(f)\boldsymbol{w}(\boldsymbol{r}_j, f)}{\sqrt{\boldsymbol{w}(\boldsymbol{r}_i, f)\boldsymbol{R}(f)\boldsymbol{w}(\boldsymbol{r}_i, f)\boldsymbol{w}(\boldsymbol{r}_j, f)\boldsymbol{R}(f)\boldsymbol{w}(\boldsymbol{r}_j, f)}}$$

Prewhitening-DICS algorithm

Use prewhitening spatial-filter weight $\boldsymbol{w}(\boldsymbol{r}_i, f)$

and prewhitening estimate of $\hat{\boldsymbol{R}}_S(f)$

The prewhitening-DICS algorithm is used in the following experiments.

DICS algorithm: J. Gross et al., Proceedings of National Academy of Science, 2001

Imaginary part of coherence

Coherence between the jth and kth voxels:

$$\eta(f, \boldsymbol{r}_j, \boldsymbol{r}_k) = \alpha(f, \boldsymbol{r}_j, \boldsymbol{r}_k) + i\beta(f, \boldsymbol{r}_j, \boldsymbol{r}_k)$$

Real part:

•Corresponds to zero time-lag correlation.

•Can be caused from non-idealistic properties of measurement system/imaging algorithm.

Imaginary part:

•Corresponds to non-zero time-lag correlation.

•Caused only by true brain interaction.

Imaginary coherence: G. Nolte et al., Clinical Neurophysiology, Vol.115, 2004

Imaging imaginary source coherence: computer simulation

Two interacting sources

Source independent from the other two sources

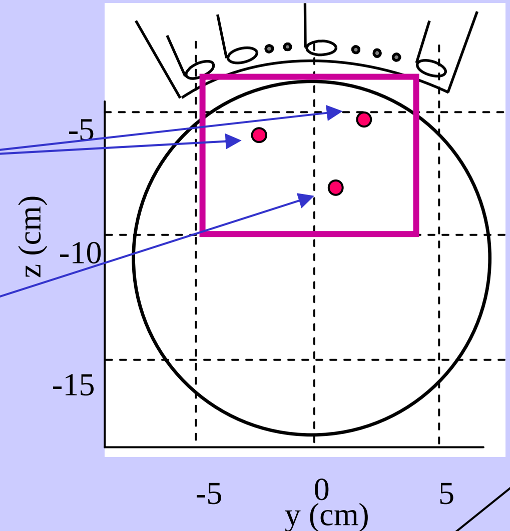

Reference voxel for coherence computation

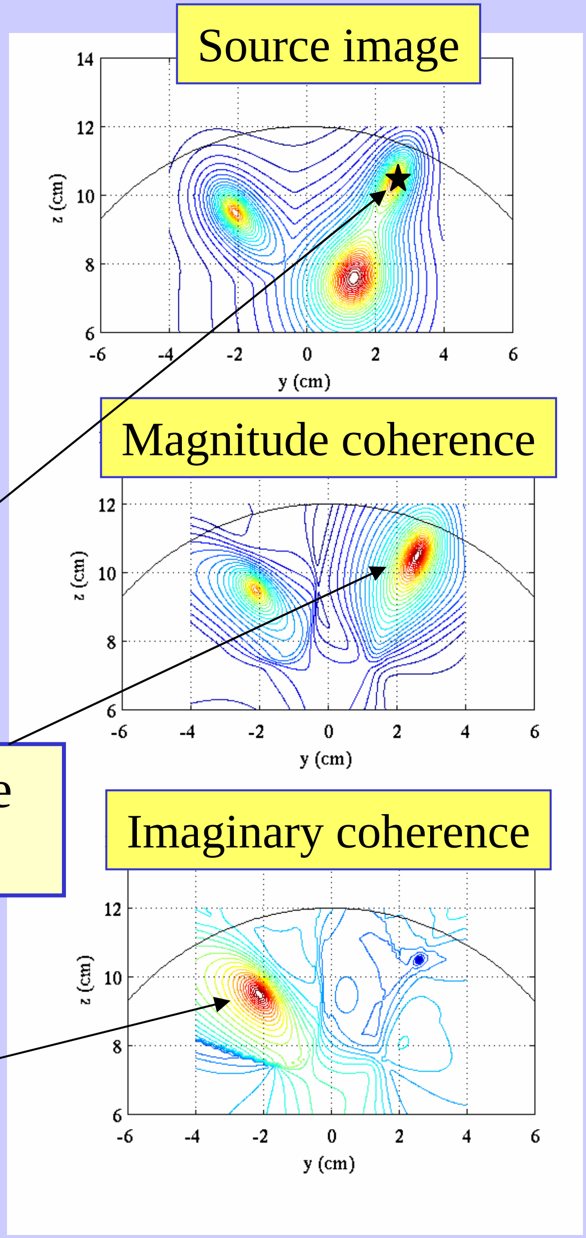

Magnitude coherence map includes spurious coherence peak caused by the blur of imaging algorithm

Imaginary coherence map represents true source interactions

Imaging source coherence: finger-tapping data

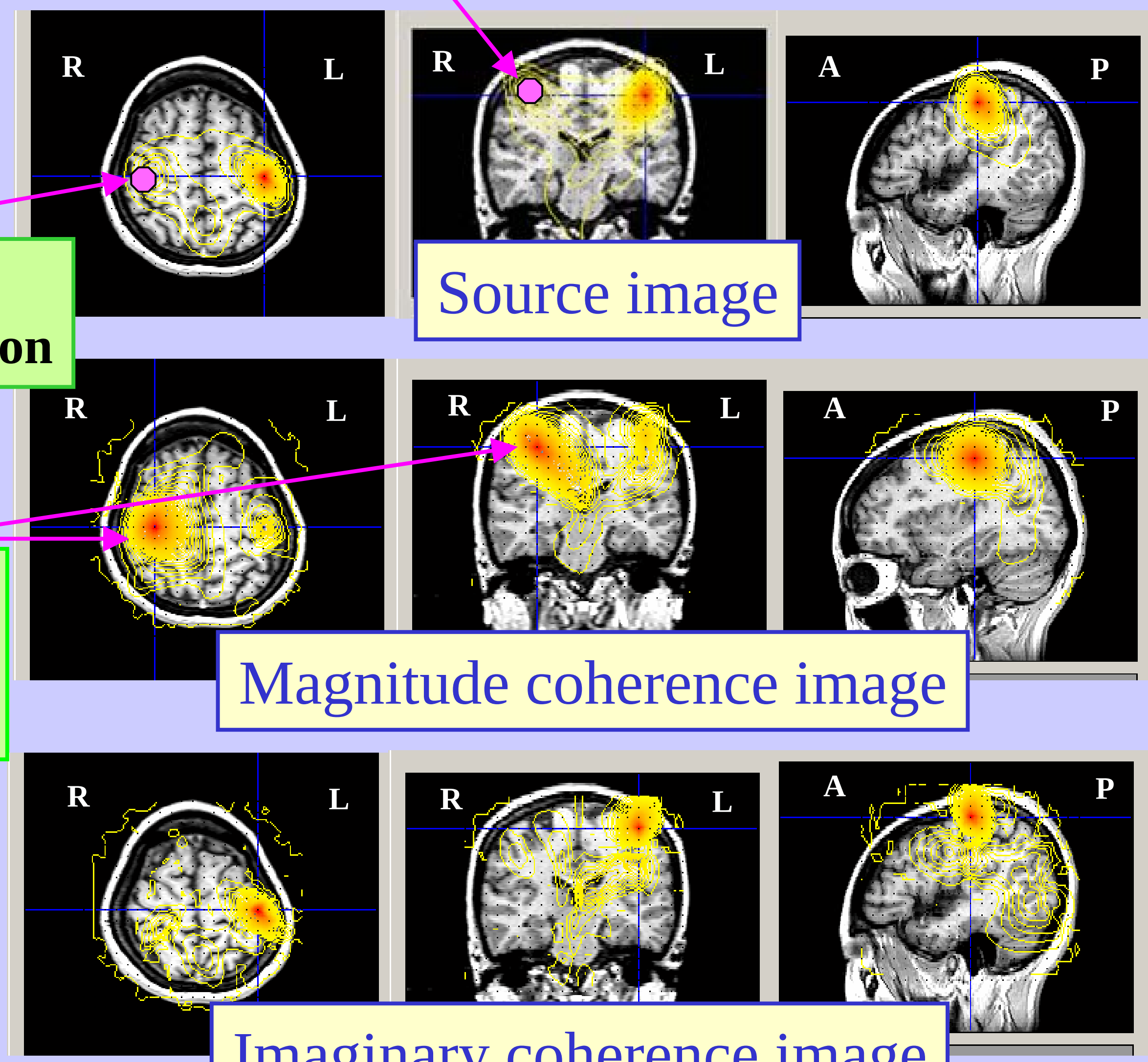

Reference point for coherence computation

Source image

Spurious coherence due to the blur of imaging algorithm

Magnitude coherence image

Imaginary coherence image

In this particular example, the spurious coherence peak is well separated from the true coherence peak and can be identified by visual inspection.

Imaging source coherence at alpha band
(Resting state MEG from a stroke patient)

Source image

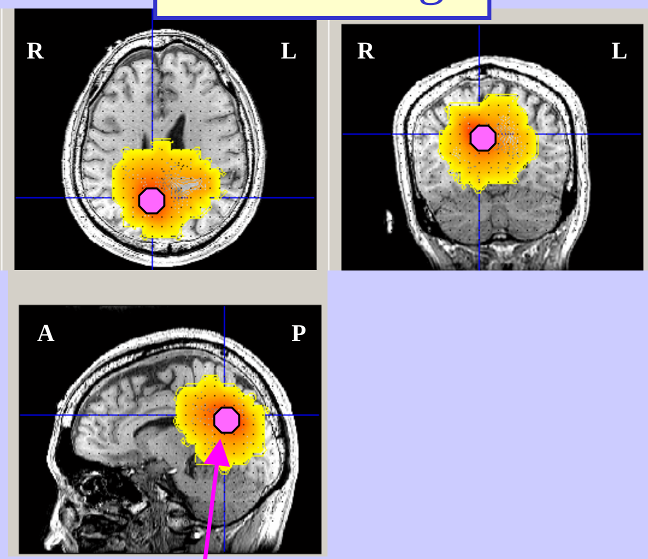

Magnitude coherence image

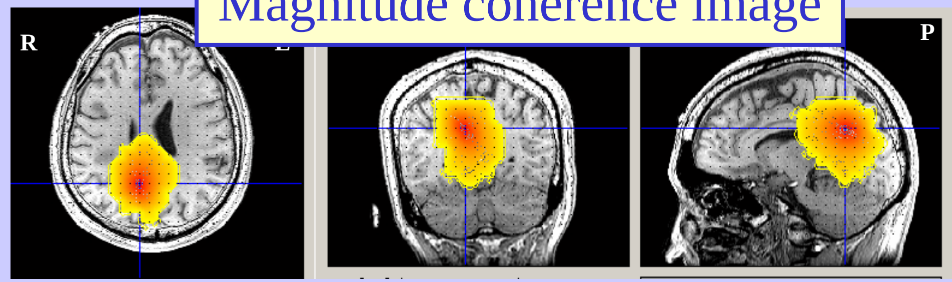

Imaginary coherence image

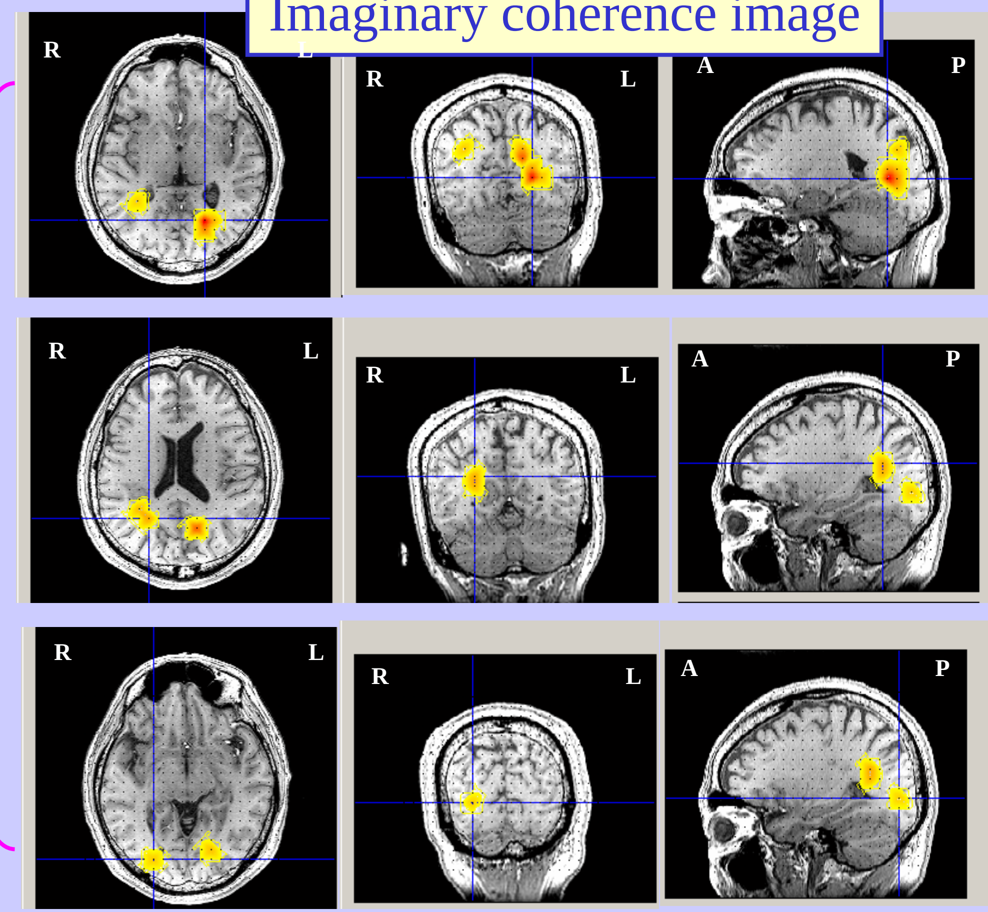

Reference point for coherence computation

Multiple sources are detected in these imaginary coherence image.

Mapping of mean imaginary coherence

Coherence between the jth and kth voxels:

$$\eta(f, \boldsymbol{r}_j, \boldsymbol{r}_k) = \alpha(f, \boldsymbol{r}_j, \boldsymbol{r}_k) + i\beta(f, \boldsymbol{r}_j, \boldsymbol{r}_k)$$

Mean imaginary coherence for the jth voxel:

$$\bar{\beta}(f, \boldsymbol{r}_j) = \tanh\left[\frac{1}{K}\sum_{k=1}^{K} \tanh^{-1} |\, \beta(f, \boldsymbol{r}_j, \boldsymbol{r}_k) \,|\right]$$

Averaged over all voxel connections
(in the Fisher's Z transform domain)

$\bar{\beta}(f, \boldsymbol{r}_j)$ represents average strength of connectivity of brain tissue at $\boldsymbol{r}_j$.

A. G. Guggisberg *et al.*, Annals of Neurology, Sep 25, 2007

Hypothesis:

•Patients with brain lesions have decreased connectivity around pathologic regions.
•Such decreased connectivity can be detected with the mean imaginary coherence at alpha band computed from resting state MEG.

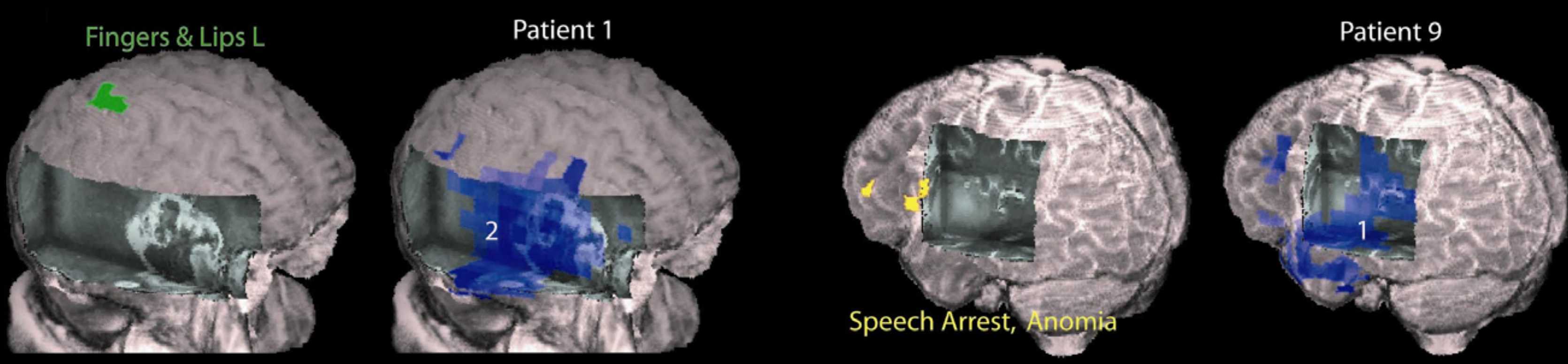

Patient #1 Patient #2

Mean-imaginary coherence can predict the functionality of pathologic brain regions in patients.

A. G. Guggisberg *et al*., Annals of Neurology, Sep 25, 2007

Mean imaginary coherence mapping for a patient with a traumatic brain damage

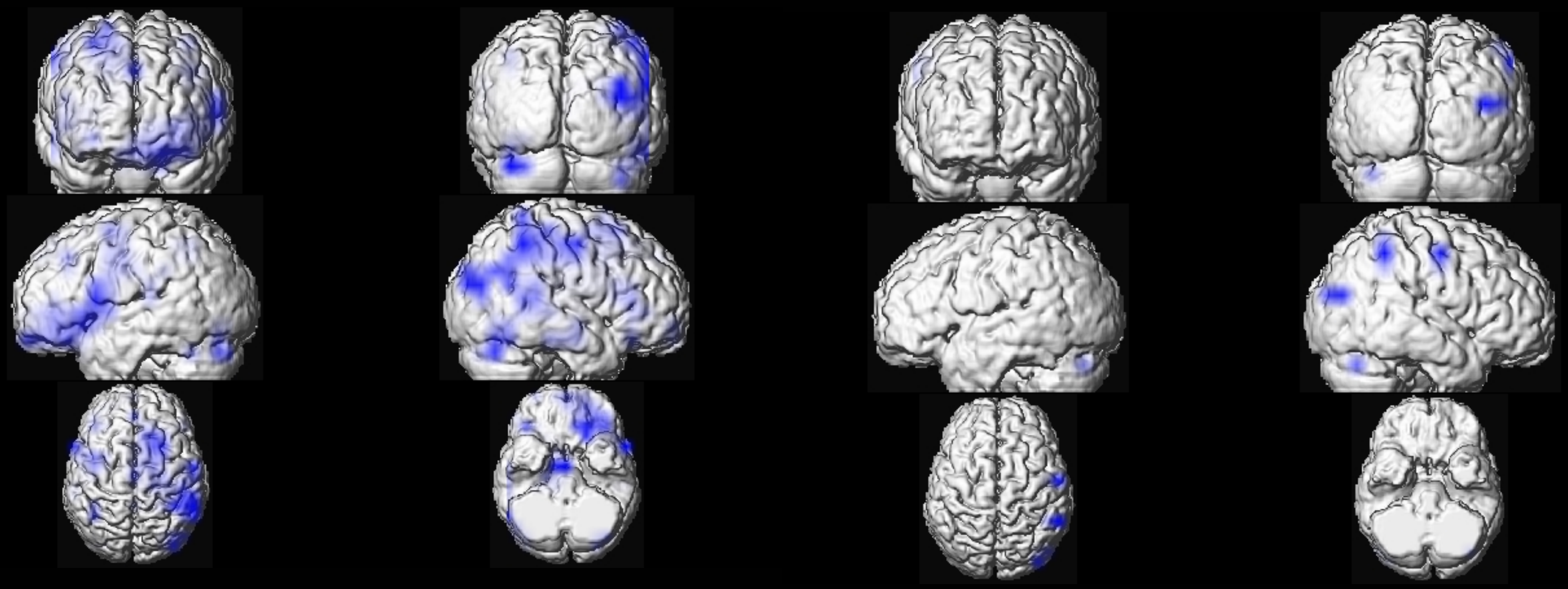

1 month after injury

2 years after injury

Mapping mean imaginary coherence can provide useful functional information on brain damage.

- Introduction of Adaptive Spatial-Filter Source Imaging

- Selected Topics on Adaptive Spatial Filters

  (1) Imaging of induced activities

  (2) Imaging of source coherence

- New Adaptive Algorithm beyond Adaptive Spatial Filters

New algorithm

Source imaging based on variational Bayesian technique

Model for Data:

Control: $\boldsymbol{b}_n = \boldsymbol{B}\boldsymbol{u}_n + \boldsymbol{v}_n$

Task: $\boldsymbol{b}_n = \boldsymbol{L}_N \boldsymbol{s}_n + \boldsymbol{B}\boldsymbol{u}_n + \boldsymbol{v}_n$

Model for Probability Distributions:

$$p(\boldsymbol{b}_n \mid \boldsymbol{s}_n, \boldsymbol{u}_n) = N(\boldsymbol{b}_n \mid \boldsymbol{L}_N \boldsymbol{s}_n + \boldsymbol{B}\boldsymbol{u}_n, \boldsymbol{\Lambda})$$

$$p(\boldsymbol{u}_n) = N(\boldsymbol{u}_n \mid 0, \boldsymbol{I})$$

$$p(\boldsymbol{s}_n) = N(\boldsymbol{s}_n \mid 0, \boldsymbol{\Phi})$$

- Built-in interference rejection capability
- Simultaneous estimation of source magnitude and orientation.
- Fast update rule for the M-step of EM algorithm

The detail of the algorithm:
In Symposium 2: Inverse Modeling and Signal Processing by Dr. Nagarajan
In Poster 7-36 by J. P. Owen

Auditory evoked field (tone burst to subject left ear)

New algorithm results

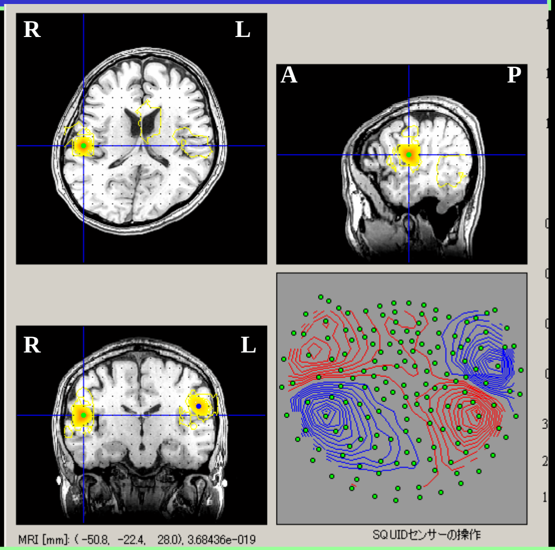

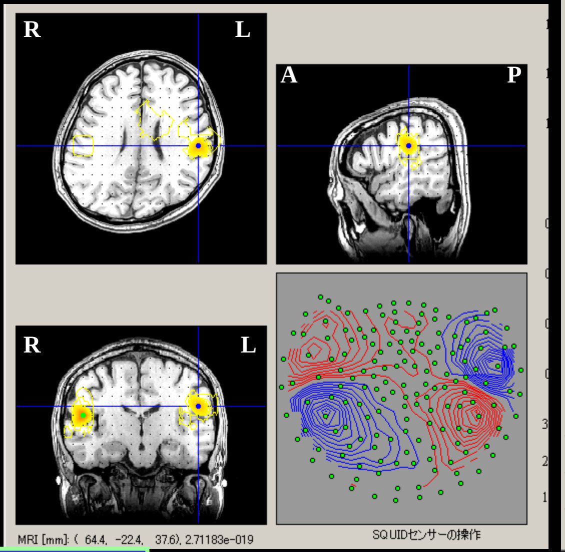

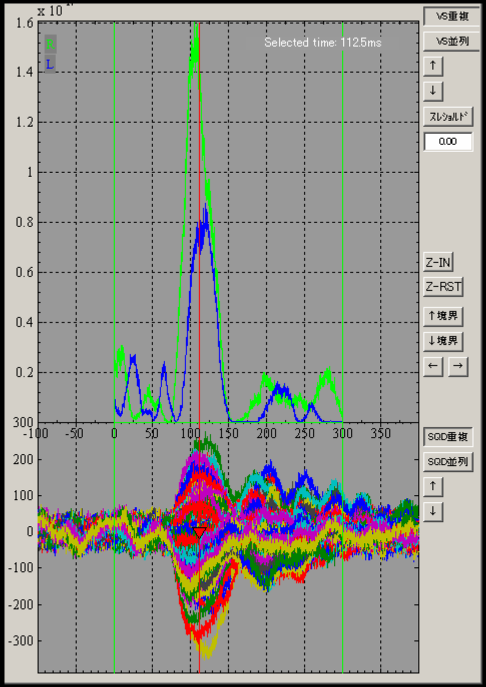

Adaptive spatial filter results

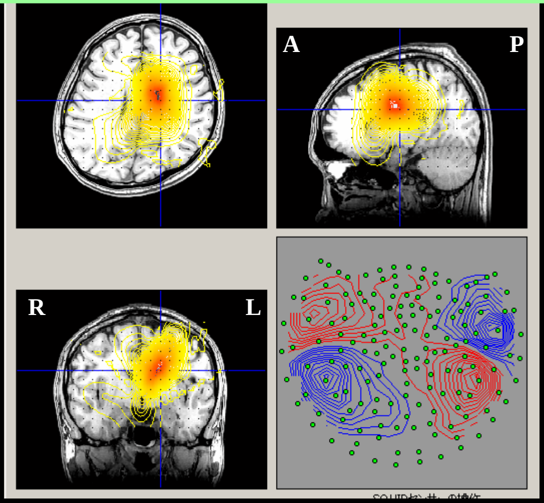

We are now conducting systematic performance evaluation on this method, and the results will be presented.

Collaborators

University of California, San Francisco

Srikantan S. Nagarajan
Anne Findlay
Sussane Honma
Sarang Dalal
Kenneth Hild II
Johanna Zumer
Hagai Atthias
David Wipf
Adrian G. Guggisberg
Julia Owen

Yokogawa Electric Ltd.

Hiroaki Tanaka
Eiichi Okumura

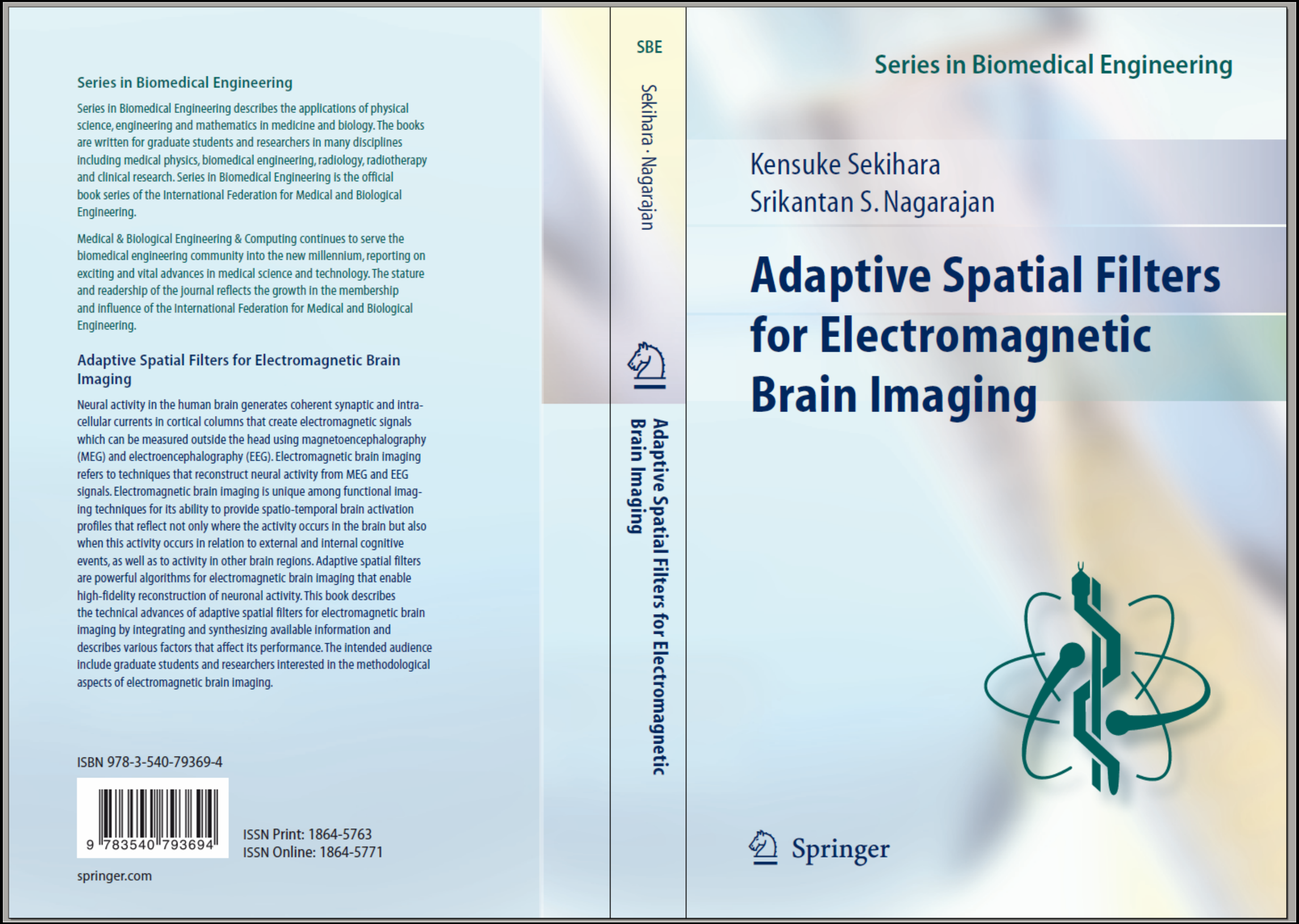

Series in Biomedical Engineering

Series in Biomedical Engineering describes the applications of physical science, engineering and mathematics in medicine and biology. The books are written for graduate students and researchers in many disciplines including medical physics, biomedical engineering, radiology, radiotherapy and clinical research. Series in Biomedical Engineering is the official book series of the International Federation for Medical and Biological Engineering.

Medical & Biological Engineering & Computing continues to serve the biomedical engineering community into the new millennium, reporting on exciting and vital advances in medical science and technology. The stature and readership of the journal reflects the growth in the membership and influence of the International Federation for Medical and Biological Engineering.

Adaptive Spatial Filters for Electromagnetic Brain Imaging

Neural activity in the human brain generates coherent synaptic and intracellular currents in cortical columns that create electromagnetic signals which can be measured outside the head using magnetoencephalography (MEG) and electroencephalography (EEG). Electromagnetic brain imaging refers to techniques that reconstruct neural activity from MEG and EEG signals. Electromagnetic brain imaging is unique among functional imaging techniques for its ability to provide spatio-temporal brain activation profiles that reflect not only where the activity occurs in the brain but also when this activity occurs in relation to external and internal cognitive events, as well as to activity in other brain regions. Adaptive spatial filters are powerful algorithms for electromagnetic brain imaging that enable high-fidelity reconstruction of neuronal activity. This book describes the technical advances of adaptive spatial filters for electromagnetic brain imaging by integrating and synthesizing available information and describes various factors that affect its performance. The intended audience include graduate students and researchers interested in the methodological aspects of electromagnetic brain imaging.

ISBN 978-3-540-79369-4

9 783540 793694

ISSN Print: 1864-5763
ISSN Online: 1864-5771

springer.com

SBE

Sekihara · Nagarajan

Adaptive Spatial Filters for Electromagnetic Brain Imaging

Series in Biomedical Engineering

Kensuke Sekihara
Srikantan S. Nagarajan

Adaptive Spatial Filters for Electromagnetic Brain Imaging

Springer

The product flyer is available at the reception desk


Thank you for your attention